RSC Advances

PAPER

View Article Online
View Journal | View Issue

Cite this: *RSC Adv.*, 2014, **4**, 21535

Three novel zinc(II) metal–organic frameworks based on three tetrazolate ligands: synthesis, structures and photoluminescence†

Hongming He,[a] Fuxing Sun,*[a] Nian Zhao,[a] Rongrong Yuan[a] and Guangshan Zhu[ab]

Received 1st April 2014
Accepted 2nd May 2014

DOI: 10.1039/c4ra02872d

www.rsc.org/advances

Three metal–organic frameworks (MOFs), namely $[Zn(BPT)H_2O]$ (**JUC-121**), $[Zn_5(IBT)_6]\cdot 8[H_2N(CH_3)_2]\cdot DMA$ (**JUC-122**) and $[Zn(TPD)(H_2O)_2]\cdot 0.5H_2O$ (**JUC-123**) (JUC = Jilin University, China), **H_2BPT** = (5-bromo-1,3-phenylene)bis(tetrazole), **H_3IBT** = 4,5-bis(tetrazol-5-yl)imidazole and **H_2TPD** = 3,5-di(tetrazol-5-yl) pyridine, were obtained by the reactions of $Zn(NO_3)_2\cdot 6H_2O$ and three tetrazolate ligands, which were characterized by single crystal X-ray diffraction, thermal gravimetric analyses (TGA), Fourier-transform infrared spectra (FT-IR), elemental analysis (CHN) and powder X-ray diffraction (PXRD). From the crystal structures of these complexes and the coordination modes of the ligands, we can see that the tetrazolate ligands have multi-connectivity abilities to obtain intriguing varieties of molecular architectures. **JUC-121** displays a three-dimensional (3D) network with the point symbol $(4\cdot 6^5)_2(4^2\cdot 8^4)(6^4\cdot 8^2)$. **JUC-122** shows a two-dimensional (2D) framework with the point symbol $(24^3)_2(24)_9$ and **JUC-123** has a 2D bimodal (3, 3)-connected net with the point symbol $(4\cdot 8^2)$. The solid-state fluorescent spectra of **JUC-121**, **JUC-122**, **JUC-123** and the free ligands were measured at room temperature.

Introduction

In the past two decades, metal–organic frameworks (MOFs),[1–3] also known as porous coordination polymers (PCPs), have attracted great interest because of intriguing varieties of molecular architectures and potential applications as functional materials.[4–17] These materials can be applied potentially in gas storage, separation,[4–7] ion exchange,[8] sensors,[9–12] heterogeneous catalysis,[13–15] optical devices[16–19] and so on. Owing to their richness and unpredictability architectures in the structural assembly of these materials, many efforts have been focused on it. The organic ligands play a significant role to tune the structures and topological networks, so a lot of organic ligands have been synthesised to prepare novel MOFs. Most of the ligands are multicarboxylic acids and aromatic N-heterocycles such as pyridine, imidazole, triazole, tetrazolate and their derivatives.[20–27] Among the ligands, tetrazolate and their derivatives as five-membered N-heterocyclic azoles have received extensive attention not only because of the richness of properties, such as spin crossover,[28,29] selective gas adsorption,[30,31] luminescent,[32] and selective ion sensing,[33] but also for their multi-connectivity abilities to obtain fascinating topological structures.

Recently, some small tetrazole linkers are applied to build up novel MOFs.[34–36] More structurally complex and functional molecular architectures and robust functionalities have been presented. To our knowledge, the largest number of exposed framework atoms (both metals and nonmetals) would likely contribute to enhanced small molecules storage capacity such as CO_2. Su *et al.* have synthesized a novel zeolite-like metal–organic framework with sodalite topology based on an N-rich tetrazolate ligand, which exhibits high CO_2 uptake and selective CO_2/N_2 adsorption capacity.[37] On the other hand, the tetrazolate ligands have multi-connectivity abilities to form very beautiful framework patterns. Evidently, it is quite interesting and challenging job to explore the assembly of N-rich tetrazolate ligand with a metal ion/cluster in crystal engineering.

Herein, we successfully designed and synthesized three small similar organic ligands with two tetrazole groups, namely, **H_2BPT** = (5-bromo-1,3-phenylene)bis(tetrazole), **H_3IBT** = 4,5-bis(tetrazol-5-yl)imidazole and **H_2TPD** = 3,5-di(tetrazol-5-yl)-pyridine. Three novel MOFs, namely $[Zn(BPT)H_2O]$ (**JUC-121**), $[Zn_5(IBT)_6]\cdot 8[H_2N(CH_3)_2]\cdot DMA$ (**JUC-122**) and $[Zn(TPD)(H_2O)_2]\cdot 0.5H_2O$ (**JUC-123**) (JUC = Jilin University, China), were synthesized by the reactions of $Zn(NO_3)_2\cdot 6H_2O$ and these ligands. Single crystal analysis demonstrates that **JUC-121**, **JUC-122** and **JUC-123** display different structures. **JUC-121** displays a

---

[a] *State Key Laboratory of Inorganic Synthesis and Preparative Chemistry, Jilin University, Changchun, 130012, P. R. China. E-mail: zhugs@jlu.edu.cn; Fax: +86-431-85168331; Tel: +86-431-85168887*

[b] *Queensland Micro- and Nanotechnology Centre, Griffith University, Queensland 4111, Australia*

† Electronic supplementary information (ESI) available. CCDC 972881–972883. For ESI and crystallographic data in CIF or other electronic format see DOI: 10.1039/c4ra02872d

three-dimensional (3D) network with the point symbol $(4\cdot6^5)_2(4^2\cdot8^4)(6^4\cdot8^2)$. **JUC-122** shows a two-dimensional (2D) framework with the point symbol $(24^3)_2(24)_9$ and **JUC-123** also has a 2D bimodal (3, 3)-connected net with the point symbol $(4\cdot8^2)$. The solid-state fluorescent spectra of free ligands, **JUC-121**, **JUC-122** and **JUC-123** were measured at room temperature.

Experimental section

Materials and methods

All the chemical reagents and solvents in this work for syntheses and analyses were purchased from commercial sources without further purification. The TGA were performed in the range of 30–800 °C under air flow at a heating rate of 10 °C min^{-1} with a Perkin-Elmer TGA thermogravimetric analyzer. Powder X-ray diffraction (PXRD) data were obtained on a Scintag X1 diffractometer at 50 kV, 200 mA for Cu-Kα ($\lambda = 1.5418$ Å) at room temperature. Elemental analyses were performed on a Perkin-Elmer 240 analyzer. Fourier-transform infrared spectroscopy (FT-IR) spectra were obtained on a Nicolet Impact 410 FT-IR spectrometer in the 4000–400 cm^{-1} range by using KBr pellets. All fluorescence measurements for the solid samples were recorded on a Fluoromax-4 spectrofluorometer at room temperature. The 300 MHz ^{1}H NMR spectra were recorded on a Bruker AV 400 spectrometer at 298 K with Me_4Si as the internal standard.

Synthesis

(5-Bromo-1,3-phenylene)bis(tetrazole) (H_2BPT). Firstly, 5-bromo-1,3-benzenedicarbonitrile was prepared according to the literature procedure.[38] A mixture of 5-bromo-1,3-benzenedicarbonitrile (1.55 g, 7.5 mmol), NaN_3 (1.95 g, 45 mmol) and triethylamine hydrochloride (6.175 g, 30 mmol) was stirred for 3 days at 100 °C in an oil-bath in a mixture system of toluene–methanol (50–10 mL). After cooling to room temperature, 40 mL of an aqueous solution of NaOH (1 M) was added dropwise over 5 minutes to the solution, which was stirred at room temperature for 1 h. Then 40 mL of diluted HCl (1 M) was added until no further white precipitate formed. The white precipitation product was collected by filtration, washed with distilled water (3 × 10 mL) and methanol (3 × 10 mL), then dried to give 1.93 g (yield: 88%). ^{1}H NMR (300 MHz, DMSO), δ (ppm): 8.76 (t, $J = 1.5$ Hz, 1H); 8.35 (d, $J = 1.4$ Hz, 2H). Selected FT-IR data (KBr pellet, cm^{-1}): 3435 (s), 3066 (m), 2942 (m), 2873 (s), 2730 (m), 2634 (s), 2520 (m), 1826 (s), 1554 (s), 1457 (s), 1386 (s), 1247 (s), 1166 (s), 1097 (s), 1008 (m), 922 (m), 887 (m), 771 (s), 736 (s), 674 (s), 524 (s), 447 (s).

4,5-Bis(tetrazol-5-yl)imidazole (H_3IBT). 4,5-Bis(tetrazol-5-yl)-imidazole (**H_3IBT**) was prepared according to the literature procedure.[39]

3,5-Di(tetrazol-5-yl)pyridine (H_2TPD). Firstly, pyridine-3,5-dicarbonitrile was prepared according to the literature procedure.[40] A mixture of pyridine-3,5-dicarbonitrile (0.97 g, 7.5 mmol), NaN_3 (1.95 g, 45 mmol) and triethylamine hydrochloride (6.175 g, 30 mmol) was added to a 100 mL flask with toluene–methanol (40–8 mL), which was stirred for 3 days with reflux. After cooling to room temperature slowly, 40 mL of an aqueous solution of NaOH (1 M) was added to the resulting solution under stirring for 1 h at room temperature. Then 1 M HCl solution was added to it to get a white precipitation with pH = 2.0–3.0. After stirring it for 1 h, the white precipitation was filtered and washed with distilled water (3 × 30 mL) to obtain 3,5-di(tetrazol-5-yl)pyridine of 1.47 g (yield: 91%). ^{1}H NMR (300 MHz, DMSO), δ (ppm): 9.37 (d, $J = 2.1$ Hz, 2H); 9.05 (t, $J = 2.1$ Hz, 1H). Selected FT-IR data (KBr pellet, cm^{-1}): 3372 (s), 3153 (s), 3064 (s), 2326 (br), 2142 (s), 1992 (s), 1914 (s), 1860 (s), 1650 (s), 1589 (s), 1448 (s), 1386 (s), 1427 (s), 1210 (m), 971 (br), 912 (s), 790 (s), 748 (s), 688 (s), 649 (s), 511 (s), 428 (s).

[Zn(BPT)H_2O] (JUC-121). A mixture of **H_2BPT** (40 mg, 0.14 mmol), $Zn(NO_3)_2\cdot6H_2O$ (60 mg, 0.2 mmol) and water–ethanol (1.6–0.4 mL) was sealed in a 20 mL Teflon-lined autoclave and heated at 130 °C for 24 h. After cooling to room temperature slowly, yellow block crystals were obtained by filtration, washed with distilled water and dried in air. Yield: 28 mg (54% based on **H_2BPT**). EA (%) calc. for $C_8H_5N_8OBrZn$: C, 25.50; H, 1.33; N, 29.75. Found: C, 25.36; H, 1.25; N, 29.21. Selected FT-IR data (KBr pellet, cm^{-1}): 3468 (br), 3056 (s), 2950 (s), 2213 (br), 1774 (s), 1712 (s), 1608 (s), 1589 (s), 1498 (s), 1442 (s), 1415 (s), 1392 (s), 1338 (s), 1259 (s), 1155 (s), 1112 (s), 1029 (br), 916 (s), 889 (s), 782 (s), 769 (s), 746 (s), 732 (s), 682 (s), 590 (br), 534 (s), 457 (s).

$[Zn_5(IBT)_6]\cdot8[H_2N(CH_3)_2]\cdot$DMA (JUC-122). A mixture of **H_3IBT** (5 mg, 0.025 mmol), $Zn(NO_3)_2\cdot6H_2O$ (15 mg, 0.05 mmol), DMA–ethanol (3.5–1.5 mL) and concentrated nitric acid was sealed into a 20 mL capped vessel. The vessel was heated at 60 °C. The crystals were obtained after 2 days, washed with DMA and dried in air. Colourless block crystals were collected. Yield: 4 mg (48% based on **H_3IBT**); EA (%) calc. for $C_{50}H_{79}N_{69}OZn_5$: C, 30.06; H, 3.96; N, 48.40. Found: C, 29.46; H, 3.26; N, 49.21. Selected FT-IR data (KBr pellet, cm^{-1}): 3442 (br), 3064 (s), 3012 (s), 2863 (br), 1625 (s), 1569 (s), 1504 (s), 1446 (s), 1409 (s), 1361 (s), 1249 (s), 1220 (s), 1186 (s), 1122 (s), 1062 (s), 1027 (m), 985 (s), 962 (s), 854 (br), 754 (s), 696 (s), 646 (s), 601 (s), 561 (s), 501 (s).

$[Zn(TPD)(H_2O)2]\cdot0.5H_2O$ (JUC-123). A mixture of **H_2TPD** (30 mg, 0.14 mmol), $Zn(NO_3)_2\cdot6H_2O$ (74 mg, 0.25 mmol) and water–ethanol (1.6–0.4 mL) was sealed in a 20 mL Teflon-lined autoclave, which was heated at 160 °C for 24 h and then cooled to room temperature, yellow block crystals were obtained by filtration, washed with distilled water, and dried in air. Yield: 34 mg (76% based on **H_2TPD**). EA (%) calc. for $C_{14}H_{16}N_{18}O_5Zn_2$: C, 25.95; H, 2.47; N, 38.93. Found: C, 25.16; H, 2.66; N, 37.93. Selected FT-IR data (KBr pellet, cm^{-1}): 3214 (br), 3083 (br), 2267 (m), 1677 (m), 1664 (m), 1452 (s), 1427 (s), 1305 (s), 1236 (s), 1207 (m), 1137 (m), 1054 (s), 1033 (s), 925 (s), 808 (s), 755 (s), 696 (s), 607 (br), 530 (s), 439 (s).

X-ray structure determination and structure refinement

Crystallographic data collections for **JUC-121**, **JUC-122** and **JUC-123** were taken on Bruker SMART APEX II CCD-based diffractometer with graphite monochromatized Mo-Kα radiation ($\lambda = 0.71073$ Å) at 298 K. Corrections for incident and diffracted beam absorption effects were applied to the date using the

Table 1 Crystal data and structure refinements for **JUC-121**, **JUC-122** and **JUC-123**

Compound	**JUC-121**	**JUC-122**	**JUC-123**
Empirical formula	$C_8H_3N_8OBr\ Zn$	$C_{30}H_6N_{60}Zn_5$	$C_{14}H_{14}N_{18}O_5Zn_2$
Formula weight	372.47	1533.90	645.21
Crystal system	Tetragonal	Hexagonal	Monoclinic
Space group	$P4_2/ncm$	$R\bar{3}c$	$P2_1/c$
a (Å)	13.280(2)	18.8708(7)	11.9967(11)
b (Å)	13.280(2)	18.8708(7)	13.2295(12)
c (Å)	13.533(3)	52.615(4)	7.0045(7)
α (°)	90.00	90.00	90.00
β (°)	90.00	90.00	90.472(1)
γ (°)	90.00	120.00	90.00
V (Å^3)	2386.7(7)	16 226.3(15)	1110.65(18)
Z	8	6	2
ρ_{calc} g cm^{-3}	2.073	0.942	1.929
μ (mm^{-1})	5.411	1.140	2.234
N_{ref}	1561	4515	2712
$F(000)$	1439.0	4533.0	648.0
$R_{(int)}$	0.0356	0.0562	0.0198
Goodness-of-fit on F^2	1.079	1.133	1.056
R_1, wR_2 [$I > 2\sigma(I)$]	0.0331, 0.0871	0.0498, 0.1621	0.0284, 0.0738
R_1, wR_2 (all data)	0.0496, 0.0954	0.0799, 0.1749	0.0373, 0.0794

SADBAS program.[41] The structures were solved by a combination of direct methods and refined by the full matrix least-squares against F^2 values using the SHELXTL program.[42] All non-hydrogen atoms were refined anisotropically and located successfully from Fourier maps. Because a large region of disordered solvent molecules in **JUC-122**, the PLATON/SQUEEZE was employed to remove their diffraction contributions.[43,44] The solvent-free structure of **JUC-122** was obtained by the SQUEEZE routine. Hydrogen atoms bonded to carbon were placed geometrically using a riding mode with an isotropic displacement parameter fixed at 1.2 times U_{eq} of the parent atoms. Hydrogen atoms of aqua or solvates of **JUC-123** were first located in difference Fourier maps and then fixed in the given positions. The detailed crystallographic data and structure refinement parameters of **JUC-121**, **JUC-122** and **JUC-123** are reported in Table 1 and the selected bond lengths and angles data are listed in Table S1,† respectively.

Results and discussion

Coordination modes of the ligands

Single crystal X-ray diffraction reveal that coordination modes of the ligands in **JUC-121**, **JUC-122** and **JUC-123** during the self-assembly process. As shown in Scheme 1, the ligands of **H_2BPT**, **H_3IBT**, and **H_2TPD** are coordinated to four, two, and three metal ions respectively and the tetrazole groups of different ligands show different coordination modes.

Crystal structure descriptions

[Zn(BPT)H_2O] (JUC-121). A single-crystal X-ray diffraction analysis reveals that **JUC-121** crystallizes in the tetragonal $P4_2/ncm$ space group and shows a 3D coordination framework. In the asymmetric unit, there is one fourth Zn1 ion, one fourth Zn2 ion, a half BPT^{2-} ligand and a half coordinated water molecule. As shown in Fig. 1a, it shows the coordination environments of Zn(II) ions. There are two independent Zn(II) ions in the structure, which adopt different geometries. Zn1 shows an octahedral ZnN4O2 with four N3 atoms (Zn1–N = 2.131 Å) originating from four tetrazolate rings of different ligands and two oxygen atoms from coordinated water molecules (Zn1–O = 2.137 Å), while Zn2 is coordinated by four N1 atoms from four tetrazoles of different ligands (Zn2–N = 2.016 Å) to form a highly distorted tetrahedral geometry. As shown in Fig. 1b and c, each BPT^{2-} ligand can be regarded as a four-bridged linker to bridge two ZnN4O2 cores and two ZnN4 cores through the 1, 3-N atoms (N1, N3) of one tetrazole to form a 3D coordination network with no any channels. Therefore, the two Zn(II) ions and the BPT^{2-} ligand can be regarded as 4-connected nodes

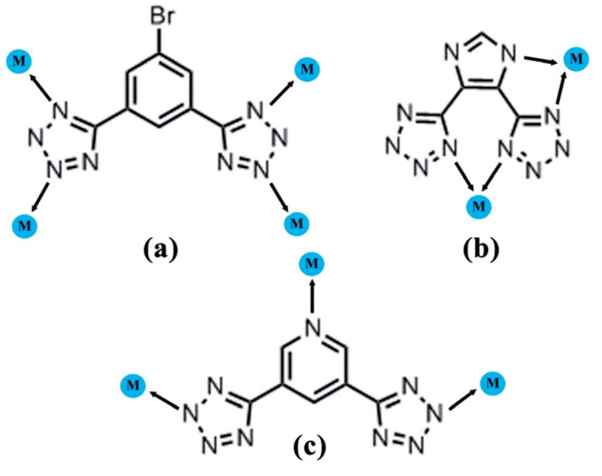

Scheme 1 The coordination modes of H_2BPT (a), H_3IBT (b) and H_2TPD (c).

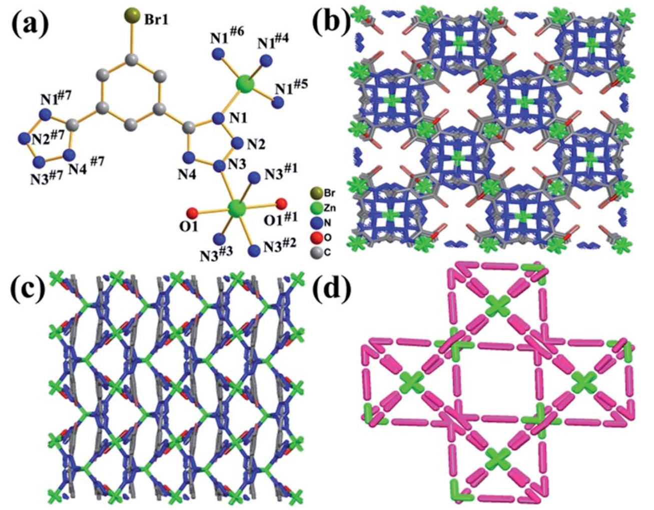

Fig. 1 (a) Coordination environments of Zn(II) atoms (symmetry code: #1 $y + 1/2, x - 1/2, -z + 2$; #2 $-x + 1, -y, -z + 2$; #3 $-y + 1/2, -x + 1/2, z$; #4 $-x + 3/2, -y + 1/2, z$; #5 $-y + 1, x - 1/2, -z + 3/2$; #6 $y + 1/2, -x + 1, -z + 3/2$; #7 y, x, z). (b) View of 3D coordination framework along the *c*-axis. (c) View of 3D coordination framework along the *a*-axis (the hydrogen atoms are omitted for clarity). (d) The simplified network of the 3D coordination framework with the point symbol $(4\cdot6^5)_2(4^2\cdot8^4)(6^4\cdot8^2)$.

topologically. The result network could be concerned a 3D network with the point symbol $(4\cdot6^5)_2(4^2\cdot8^4)(6^4\cdot8^2)$.

$[Zn_5(IBT)_6]\cdot8[H_2N(CH_3)_2]\cdot$DMA (JUC-122). X-ray crystallography confirms that **JUC-122** has a 2D framework and crystallizes in the hexagonal $R\bar{3}c$ space group. There is one third Zn1 ion, one second Zn2 ion and one IBT^{3-} ligand in the asymmetric unit. There are two crystallographically different Zn(II) (Fig. 2a). The Zn1 ion is bound with six nitrogen atoms, which are three pairs of N1 and N5 atoms from three independent IBT^{3-} ligands to form a distorted octahedral geometry (Zn1–N = 2.162 Å). Meanwhile, the Zn2 ion exhibits a distorted tetrahedral ZnN4 geometry with two pairs of N4 and N10 atoms belonging to the tetrazolate rings from two independent IBT^{3-} ligands (Zn2–N = 1.982–1.990 Å). Each IBT^{3-} ligand connects with two Zn(II) ions to form a 2D framework (Fig. 2b) with triangular lattice, involving twelve ligands and twelve Zn(II) ions. The 2D networks are packed together with ABC fashion by weak intermolecular van der Waals interactions to form a 3D supramolecular architecture (Fig. 2c and d). The guest solvent molecules included in the frameworks could be refined, which can be confirmed by the TGA and elemental analyses. From the topologic point of view, the Zn1 ion, Zn2 ion can be regarded as 3-connected and 2-connected nodes, respectively, and the ligand can be simplified into a 2-connected linker to achieve a 2D network with the point symbol $(24^3)_2(24)_9$ (Fig. 2e). This topology can be regarded as one augmented form of honeycomb (hcb) topology.

$[Zn(TPD)(H_2O)_2]\cdot0.5H_2O$ (JUC-123). The X-ray crystallographic study shows that **JUC-123** crystallizes in the monoclinic space group $P2_1/c$ and possesses a 2D framework. The asymmetric unit of **JUC-123** contains one Zn ion, one TPD^{2-} ligand, two coordinated water molecules and a half guest water molecule. Each Zn(II) is five-coordinated by N2, N5 and N7 from three different ligands (Zn–N = 2.003–2.059 Å) and two oxygen atoms originating from two coordinated water molecules (Zn–O = 2.149–2.154 Å) (Fig. 3a). Each ligand is deprotonated to furnish a TPD^{2-} anion, which links three Zn ions in a three-bridged fashion to yield a 2D supramolecular layer (Fig. 3b). As shown in Fig. 3c and d, the 2D layers are packed together with AB fashion by π–π stacking between arene cores of two independent TPD^{2-} (3.611 Å) and weak intermolecular van der Waals interactions to yield a 3D framework. Topologically, by considering TPD^{2-} anions and Zn(II) ions as 3-connected nodes, the 2D framework can be symbolized as a (3, 3)-connected net with the point symbol $(4\cdot8^2)$ (Fig. 3e).

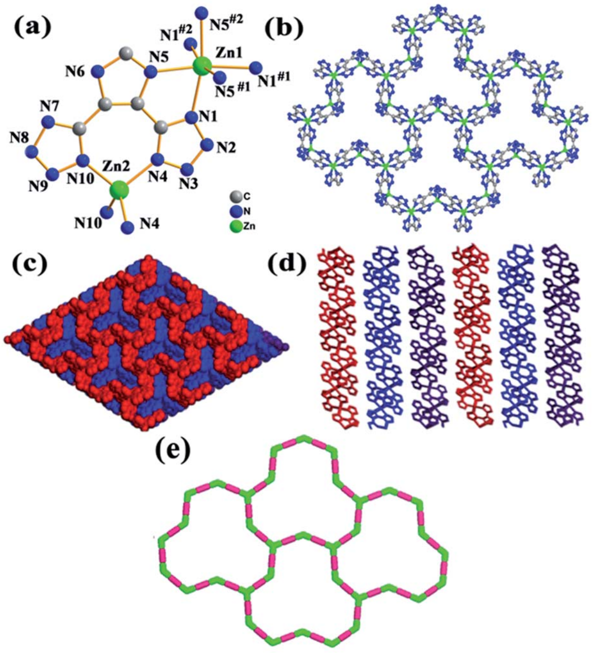

Fig. 2 (a) Coordination environments of Zn(II) atoms (symmetry code: #1 $-y, x - y, z$; #2 $-x + y, -x, z$; #3 $x - y + 1/3, -y + 2/3, -z + 1/6$). (b) View of the single 2D network along the *c*-axis. (c) View of the packed layers of **JUC-122** along the *c*-axis. (d) The 2D networks are packed together with ABC fashion to form a 3D supramolecular architecture along the *b*-axis (the hydrogen atoms and solvent molecules are omitted for clarity). (e) The simplified network of the single 2D network along the *c*-axis with the point symbol $(24^3)_2(24)_9$.

Thermal analysis

PXRD analyses of **JUC-121**, **JUC-122** and **JUC-123** were carried out at room temperature (Fig. 4a and c). The results show that the experimental PXRD patterns are closely matched those in the simulated patterns from single crystal structures, which reveal that the phase purity of the bulk crystalline materials. From the thermal gravimetric analyses (Fig. 4d), **JUC-121** shows a slow weight loss of 4.89% (calculated: 4.78%) in the range 30–280 °C, corresponds to loss one coordinated water molecule. Upon further heating, the framework decomposed gradually at 380 °C. The TGA of **JUC-122** exhibits an initial weight loss 23.23% (calculated: 23.15%) before 157 °C and the framework collapsed at 300 °C. **JUC-123** losses a half guest and two

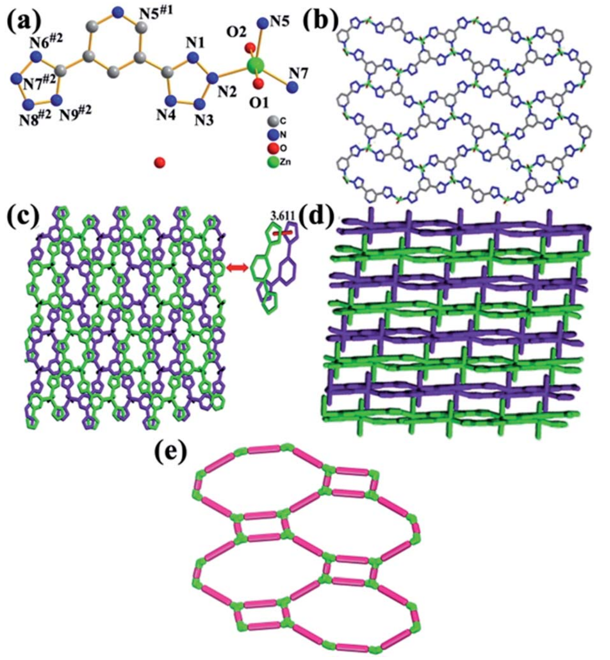

Fig. 3 (a) Coordination environment of Zn(II) atoms (symmetry code: #1 −*y*, −*y*, −*z*; #2 *x* − 1, −*y* + 0.5, *z* − 0.5). (b) View of the single 2D network along the *c*-axis. (c) View of the packed double-layers of **JUC-123** along the *c*-axis. (d) The 2D networks are packed together with AB fashion to form a 3D framework along the *b*-axis. (the hydrogen atoms and solvent molecules are omitted for clarity). (e) The simplified network of the single 2D network along the *c*-axis with a 2D bimodal (3, 3)-connected net with the point symbol $(4\cdot8^2)$.

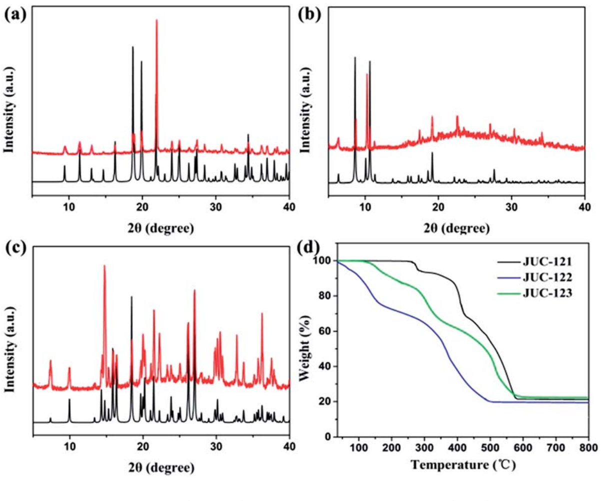

Fig. 4 The simulated (black) and as-synthesized (red) powder X-ray diffraction of **JUC-121** (a), **JUC-122** (b) and **JUC-123** (c). (d) The TGA curves of **JUC-121**, **JUC-122** and **JUC-123**.

terminal water molecules before 270 °C, which is about 15.73% (calculated: 13.91%).

Photoluminescence properties

The solid-state luminescent properties of the free ligands, **JUC-121**, **JUC-122** and **JUC-123** were measured at room temperature.

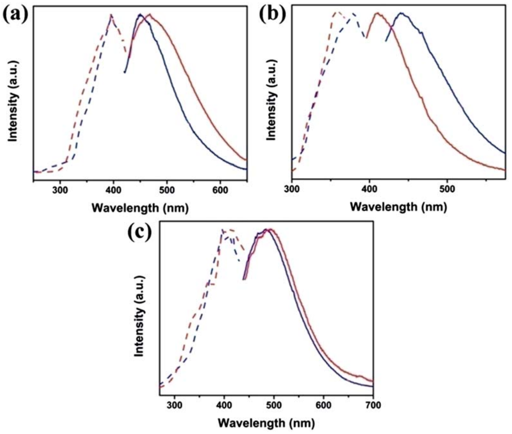

Fig. 5 Excitation (dot lines) and emission (solid lines) spectra of (a) H_2BPT (blue) and **JUC-121** (red), (b) H_3IBT (blue) and **JUC-122** (red), (c) H_2TPD (blue) and **JUC-123** (red).

As shown in Fig. 5, a broad photoluminescence emission band at 452, 440 and 480 nm under an excitation of 397, 380 and 396 nm for the **H_2BPT**, **H_3IBT**, **H_2TPD** ligands, respectively, which are probably attributable to the $\pi^* \rightarrow \pi$ or $\pi^* \rightarrow n$ transitions.[45,46] The luminescence properties of **JUC-121**, **JUC-122** and **JUC-123** in the solid state were also investigated at room temperature. These complexes show emission bands at 468 nm ($\lambda_{em} = 396$ nm) for **JUC-121**, 412 nm ($\lambda_{em} = 356$ nm) for **JUC-122** and 495 nm ($\lambda_{em} = 411$ nm) for **JUC-123**, respectively. Compared to the excitation and emission spectra of the free ligands, the observed emissions of **JUC-121** and **JUC-123** are red-shifted 16 nm and 15 nm, respectively. It indicates that the luminescent properties are mainly attributed to the intraligand transition and ligand-to-metal, which are in good agreement with literature examples on this class of Zn(II) coordination compounds.[47,48] Furthermore, **JUC-122** is different from the others. The emission band of **JUC-122** exhibits blue-shifted 28 nm, which may be presumably attributed to the coordination of the IBT^{3-} ligand to the central Zn(II) ions. It leads to less vibrations of the skeleton and reduces the loss of energy by radiationless decay of the intraligand emission excited state.[49,50]

Conclusions

In summary, three novel metal–organic frameworks based on Zn(II) and three different tetrazolate ligands were synthesized. **JUC-121** features a 3D supramolecular network with the point symbol $(4\cdot6^5)_2(4^2\cdot8^4)(6^4\cdot8^2)$. Meanwhile, **JUC-122** exhibits a 2D network with the point symbol $(24^3)_2(24)_9$ and **JUC-123** has a 2D bimodal (3, 3)-connected net with the point symbol $(4\cdot8^2)$. From the crystal structures of these complexes and the coordination modes of the ligands, the four N atoms of the tetrazolate and their derivatives all have good coordination abilities with metal ions to generate unpredictable structures and fascinating topologies. It is expected that more extensive researches to explore and develop more kinds of ligands with tetrazole groups to generate the richness and unpredictability of structures and topologies.

Acknowledgements

We are grateful to the financial support from National Basic Research Program of China (973 Program, grant nos 2012CB821700, grant nos 2014CB931804), Major International (Regional) Joint Research Project of NSFC (grant nos 21120102034), NSFC (grant nos 20831002) and the Australian Research Council Future Fellowship (FT100101059).

Notes and references

1 M. Li, D. Li, M. O'Keeffe and O. M. Yaghi, *Chem. Rev.*, 2014, **114**, 1343.

2 J. R. Long and O. M. Yaghi, *Chem. Soc. Rev.*, 2009, **38**, 1213.

3 L. E. Kreno, K. Leong, O. K. Farha, M. Allendorf, R. P. Van Duyne and J. T. Hupp, *Chem. Rev.*, 2012, **112**, 1105.

4 S. Horike, Y. Inubushi, T. Hori, T. Fukushima and S. Kitagawa, *Chem. Sci.*, 2012, **3**, 116.

5 P.-Z. Li, X.-J. Wang, R. H. D. Tan, Q. Zhang, R. Zou and Y. Zhao, *RSC Adv.*, 2013, **3**, 15566.

6 C. E. Wilmer, O. K. Farha, Y.-S. Bae, J. T. Hupp and R. Q. Snurr, *Energy Environ. Sci.*, 2012, **5**, 9849.

7 J. Qian, F. Jiang, L. Zhang, K. Su, J. Pan, Q. Li, D. Yuan and M. Hong, *Chem. Commun.*, 2014, **50**, 1678.

8 Z. Zhang, L. Zhang, L. Wojtas, P. Nugent, M. Eddaoudi and M. J. Zaworotko, *J. Am. Chem. Soc.*, 2012, **134**, 924.

9 Z. Jin, H. He, H. Zhao, T. Borjigin, F. Sun, D. Zhang and G. Zhu, *Dalton Trans.*, 2013, **42**, 13335.

10 J. He, M. Zha, J. Cui, M. Zeller, A. D. Hunter, S.-M. Yiu, S.-T. Lee and Z. Xu, *J. Am. Chem. Soc.*, 2013, **135**, 7807.

11 W. Yang, Z.-Q. Bai, W.-Q. Shi, L.-Y. Yuan, T. Tian, Z.-F. Chai, H. Wang and Z.-M. Sun, *Chem. Commun.*, 2013, **49**, 10415.

12 D. Banerjee, Z. Hu, S. Pramanik, X. Zhang, H. Wang and J. Li, *CrystEngComm*, 2013, **15**, 9745.

13 L. Lili, Z. Xin, R. Shumin, Y. Ying, D. Xiaoping, G. Jinsen, X. Chunming and H. Jing, *RSC Adv.*, 2014, **4**, 13093.

14 D. Farrusseng, S. Aguado and C. Pinel, *Angew. Chem., Int. Ed.*, 2009, **48**, 7502.

15 D. Jiang, A. Urakawa, M. Yulikov, T. Mallat, G. Jeschke and A. Baiker, *Chem.–Eur. J.*, 2009, **15**, 12255.

16 H. He, F. Sun, T. Borjigin, N. Zhao and G. Zhu, *Dalton Trans.*, 2014, **43**, 3716.

17 C. X. Chen, Q. K. Liu, J. P. Ma and Y. B. Dong, *J. Mater. Chem.*, 2012, **22**, 9027.

18 M.-L. Ma, C. Ji and S.-Q. Zang, *Dalton Trans.*, 2013, **42**, 10579.

19 H. Zhang, P. Lin, X. Shan, F. Du, Q. Li and S. Du, *Chem. Commun.*, 2013, **49**, 2231.

20 H.-D. Guo, D.-F. Qiu, X.-M. Guo, G.-L. Zheng, X. Wang, S. Dang and H.-J. Zhang, *CrystEngComm*, 2009, **11**, 2425.

21 H. He, F. Sun, H. Su, J. Jia, Q. Li and G. Zhu, *CrystEngComm*, 2014, **16**, 339.

22 X.-C. Huang, Y.-Y. lin, J.-P. Zhang and X.-M. Chen, *Angew. Chem., Int. Ed.*, 2006, **45**, 1557.

23 S. Biswas, M. Grzywa, H. P. Nayek, S. Dehnen, I. Senkovska, S. Kaskel and D. Volkmer, *Dalton Trans.*, 2009, 6487.

24 S. Horike, M. Dincă, K. Tamaki and J. R. Long, *J. Am. Chem. Soc.*, 2008, **130**, 5854.

25 C. Jiang, Z. Yu, C. Jiao, S. Wang, J. Li, Z. Wang and Y. Cui, *Eur. J. Inorg. Chem.*, 2004, 4669.

26 Y.-X. Tan, Y.-P. He, M. Wang and J. Zhang, *RSC Adv.*, 2014, **4**, 1480.

27 B. Xu, Q.-S. Liang, L.-T. Liu, Q.-S. Liu and C.-C. Li, *RSC Adv.*, 2014, **4**, 13919.

28 Z. Song, H. Gao, G. Li, Y. Yu, Z. Shi and S. Feng, *CrystEngComm*, 2009, **11**, 1579.

29 M. Zhu, S.-Q. Su, X.-Z. Song, Z.-M. Hao, S.-Y. Song and H.-J. Zhang, *Dalton Trans.*, 2012, **41**, 13267.

30 B. Ding, L. Yi, P. Cheng, D. Z. Liao and S. P. Yan, *Inorg. Chem.*, 2006, **45**, 5799.

31 R. Poloni, B. Smit and J. B. Neaton, *J. Am. Chem. Soc.*, 2012, **134**, 6714.

32 J. Y. Sun, D. J. Zhang, L. Wang, Y. Cao, D. Li, L. Y. Zhang, W. Song, Y. Fan, J. N. Xu and T.-Y. Song, *CrystEngComm*, 2012, **14**, 3982.

33 H. Lee, S. H. Jung, W. S. Han, J. H. Moon, S. Kang, J. Y. Lee, J. H. Jung and S. Shinkai, *Chem.–Eur. J.*, 2011, **17**, 2823.

34 D.-C. Zhong, J.-H. Deng, X.-Z. Luo, T.-B. Lu and K.-J. Wang, *CrystEngComm*, 2012, **14**, 1538.

35 F. Wang, D.-C. Hou, H. Yang, Y. Kang and J. Zhang, *Dalton Trans.*, 2014, **43**, 3210.

36 T. Hu, W. Bi, X. Hu, X. Zhao and D. Sun, *Cryst. Growth Des.*, 2010, **10**, 3325.

37 J.-S. Qin, D.-Y. Du, W.-L. Li, J.-P. Zhang, S.-L. Li, Z.-M. Su, X.-L. Wang, Q. Xu, K.-Z. Shao and Y.-Q. Lan, *Chem. Sci.*, 2012, **3**, 2114.

38 T. J. Doyle and J. Haseltine, *J. Heterocycl. Chem.*, 1994, **31**, 1417.

39 M. Dincă, T. D. Harris, A. T. lavarone and J. R. Long, *J. Mol. Struct.*, 2008, **890**, 139.

40 N. Kanomata, H. Nagahara and M. Tada, *JJ. Heterocycl. Chem.*, 1992, **29**, 1567.

41 G. M. Sheldrick, *SADABS, Program for Empirical Absorption Correction for AreaDetector Data*, University of Gottingen, Gottingen, Germany, 1996.

42 G. M. Sheldrick, *SHELXTL Version 5.1 Software Reference Manual*, Bruker AXS. Inc., Madison, WI1997.

43 A. L. Spek, *J. Appl. Crystallogr.*, 2003, **36**, 7.

44 A. L. Spek, *PLATON, A multipurpose crystallographic tool*, Utrecht University, The Netherlands, 2001.

45 X. Shi, G. Zhu, Q. Fang, G. Wu, G. Tian, R. Wang, D. Zhang, M. Xue and S. Qiu, *Eur. J. Inorg. Chem.*, 2004, 185.

46 H.-Y. Bai, J.-F. Ma, J. Yang, Y.-Y. Liu and J.-C. Ma, *Cryst. Growth Des.*, 2010, **10**, 995.

47 M. D. Allendorf, C. A. Bauer, R. K. Bhakta and R. J. T. Houk, *Chem. Soc. Rev.*, 2009, **38**, 1330.

48 Y. Cui, Y. Yue, G. Qian and B. Chen, *Chem. Rev.*, 2012, **112**, 1126.

49 A. Thirumurugan and S. Natarajan, *Dalton Trans.*, 2004, **18**, 2329.

50 L.-Y. Zhang, G.-F. Liu, S.-L. Zheng, B.-H. Ye, X.-M. Zhang and X.-M. Chen, *Eur. J. Inorg. Chem.*, 2003, **16**, 2965.